Quiet and noisy metastable voltage states in high-T_c superconductors

G. Jung*

Department of Physics, Ben Gurion University of the Negev, P.O. Box 653, 84105 Beer-Sheva, Israel

B. Savo

Dipartimento di Fisica and INFM, Università di Salerno, 84081 Baronissi (SA), Italy

Y. Yuzhelevski

Department of Physics, Ben Gurion University of the Negev, P.O. Box 653, 84105 Beer-Sheva, Israel

The interaction between the telegraph noise and background voltage fluctuations in the current induced dissipative state of high-T_c BiSrCaCuO thin films has been investigated. Experimental time records of the voltage drop across current biased thin film strips show markedly different background noise traces in the up and down telegraph states. Detailed analysis demonstrates that fluctuations around the telegraph voltage levels are due to a unique background noise process. The apparent quiet and noisy voltage states are due only to differences in the effective frequency bandwidth at which background noise is seen at distinct telegraph levels. Changes of the background noise variance ratio with changing bias current follow changes of the statistical average lifetimes of the random telegraph process.

I. INTRODUCTION

Voltage noise in the thermodynamically superconducting state is associated with dissipation induced by motion of magnetic flux structures and/or action of intrinsic Josephson junctions. In good quality high-T_c superconducting (HTSC) samples the dissipation caused by the flow of transport currents along the superconducting planes is dominated by dissipative flux processes. Flux noise due to randomness in vortex matter dynamics converts into observable voltage fluctuations by means of an intrinsic flux-to-voltage conversion mechanism.[1–3] Low frequency flux and voltage noise in HTSC systems typically appears as wide band Gaussian fluctuations with a $1/f$-like power spectral density (PSD). $1/f$-like noise is frequently accompanied by characteristic non-Gaussian random telegraph noise (RTN) components. Telegraph signals in HTSC systems were detected in magnetic flux noise at low[5–7] and high magnetic fields,[8] magnetically modulated microwave absorption,[9] and in voltages appearing across dc current biased thin films.[3,10–14]

In the simplest case of a two-level random telegraph signal (dichotomous noise) the observable switches randomly between two fixed levels, referred to as ''up'' and ''down'' level. Generation of dichotomous noise can generally be traced to an action of a two-level fluctuator (TLF) consisting of two energy wells separated by a barrier. The system undergoes thermally activated or tunnel transitions between the wells corresponding to random switching of the measured observable, for a review see Ref. 4. In reality, random telegraph signals deviate from the ideal two-level fluctuator picture. First of all, experimentally observed RTN always appears on the background of noise contributed by other random processes in the sample and by instruments in the electronics chain. Waveforms of experimentally observed HTSC random telegraph signals frequently exhibit exotic features, such as multilevel switching[5,7,15] and modulation of

telegraph amplitude and/or switching frequency by yet another telegraph signal.[16,17]

Among many exotic manifestations of RTN signals in HTSC systems, events demonstrating different traces of background noise at different RTN levels, or in other words, background noise which changes synchronously with the telegraph signal, deserves particular attention. This phenomenon was first observed in flux noise experiments performed at zero field cooled HTSC samples and since then is referred to as ''noisy and quiet metastable states.''[5] Pronounced asymmetry in the background noise variance at distinct telegraph levels has subsequently been observed by us in the voltage noise of current biased HTSC thin films.[16] The appearance of quiet and noisy telegraph states was tentatively interpreted as a signature of vortex hopping from a site where it is relatively mobile to a site where it is much more restricted spatially.[5] This assumption imposes strong conditions on the model of an active two-level fluctuator by requiring the TLF energy wells to have different curvature. Consequently, the attempt frequencies for two distinct wells must also be assumed to be different. Thus a TLF responsible for the appearance of quiet and noisy metastable states deviates markedly from the classical TLF scenario of two symmetric wells separated by an asymmetric barrier.[4,19]

It is worth remembering here that similar exotic random telegraph wave forms have been observed in nonsuperconducting solid state systems.[18–21] The nonsuperconducting quiet and noisy RTN events were generally ascribed to interactions between localized structural defects and active two-level fluctuators in small size systems. Nevertheless, mechanisms responsible for synchronous switching of RTN level and background noise intensity as well as modulation of the telegraph wave forms in HTSC samples cannot be consistently explained by evoking similar defect-fluctuator interactions.[5] This paper is devoted to the experimental investigation of the nature of quiet and noisy metastable states
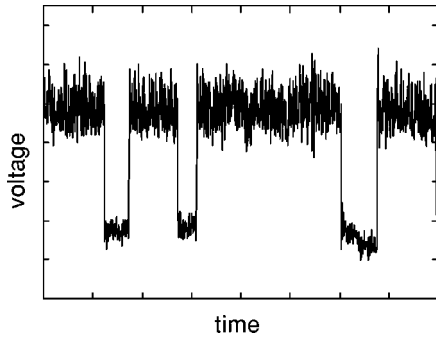
FIG. 1. A typical telegraph noise time record demonstrating quiet (down level) and noisy (up level) metastable states.
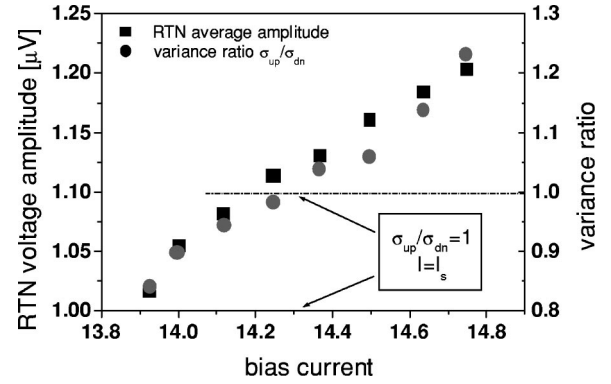

FIG. 2. Current dependence of the variance ratio (left axis) and RTN amplitude (right axis) recorded at zero applied magnetic field in current induced dissipative state (zero cooled sample) at 77 K. Note that $\sigma_{up}/\sigma_{dn}=1$ for $I=I_s=14.3$ mA.

appearing in random telegraph voltage noise in zero field cooled BiSrCaCuO thin film strips which are driven into a dissipative state by dc current flow.

II. EXPERIMENTAL

The experiments were performed with 300 nm thick, c-axis oriented high quality thin BiSrCaCuO 2212 films fabricated by means of molecular beam epitaxy. The details of sample preparation and characterization are reported elsewhere.[22] The films had a very high residual resistance ratio, $R_{300/100}\geq 3.3$, $T_c(R=0)$ above 86 K, and critical current density $J_c(4.2$ K$)\sim 10^5$ A/cm^2. X-ray diffraction spectra of the films showed only peaks of the pure 2212 phase and strong preferential orientation with the c axis perpendicular to the substrate plane. The films were patterned into 50 μm wide strips with large silver covered contacts pads on both ends of the strip and voltage pick-up leads separated by 50 μm. In the experiments the voltage signal developed under dc current flow in the strip was delivered to the top of cryostat, amplified by a low noise preamplifier, and processed by a signal analyzer. Several random telegraph events were detected in many, relatively narrow, noisy window ranges of temperature, current flow and associated magnetic fields. In this paper we concentrate, however, only on RTN events observed in the current induced dissipative state at zero applied magnetic field.

An example of a RTN wave form appearing in one of our strips at 77 K is shown in Fig. 1. Even a brief examination of the experimental record convinces one that the apparent background noise intensities at distinct telegraph levels are markedly different. This is a clear manifestation of the quiet and noisy metastable states seen in the form of voltage fluctuations. It should be emphasized that the appearance of quiet and noisy metastable states in current biased HTSC samples is not restricted to a particular type of a sample or deposition technique. We have previously reported similar events in BSCCO films obtained by liquid phase epitaxy on NdGaO$_3$ substrates.[16]

The switching in the intensity of the background noise synchronous with the RTN signal suggests that some form of statistical correlations between RTN and background fluctuations may exist. To get a deeper insight into this puzzling phenomenon we have performed a detailed statistical analysis of the RTN wave forms and background fluctuations. The experimentally observed background noise has been investigated by analyzing Gaussian distributions of voltage fluctuations around mean voltages of the RTN levels. For each current flow the analysis was performed by averaging the results of at least five time records sampled in 40 960 points. The RTN components of the experimental record have been initially analyzed by annotating the time instances at which the system undergoes transitions between RTN states, determining the time lengths of individual pulses and heights of individual RTN amplitudes, building their histograms, and finding the statistical average values. This procedure is straightforward for clean RTS signals, well above the background noise intensities. However, this approach fails completely in the case of ''noisy'' records, for which it becomes difficult to determine the precise moment at which transitions occur. To enable analysis of the experimental records strongly perturbed by the background noise we have developed a new procedure of RTN analysis in the time domain which is based on differences between statistical properties of the Gaussian background noise and Marcovian RTN fluctuations (Sec. III).

Statistical analysis confirmed that variances of background fluctuations around up and down telegraph levels are indeed different. Moreover, we have found that the ratio between variances σ_{up}/σ_{dn} changes markedly with changing current flow, as shown in Fig. 2. The dependence of the variance ratio on bias current should not be surprising, since all statistical average parameters of the RTN fluctuations in HTSC systems are known to change with changing current flow.[3,10–12,14] The evolution of RTN lifetimes with changing bias current as determined from experimental records is illustrated in Fig. 3, while the current dependence of RTN amplitude is plotted in Fig. 2 together with the variance ratio.

Figure 2 shows that current induced changes of the variance ratio follow closely the RTN amplitude evolution. This feature may be evoked as an argument in the favor of possible statistical correlation between RTN and background fluctuations. However, a careful examination of the variance ratio behavior reveals that at a certain current flow, the variances of the background noise at RTN levels become equal, $\sigma_{up}=\sigma_{dn}$. Moreover, one finds that with further current increase the noisy and quiet metastable states are interchanged. The current flow at which the variances become equal corresponds to the symmetrizing current I_s at which $\tau_{up}=\tau_{dn}$
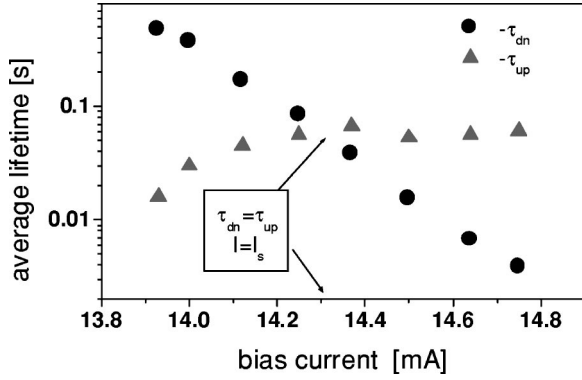
FIG. 3. The evolution of average RTN lifetimes with changing bias current. Note that for the symmetrizing current $I = I_s$ the RTN wave form is symmetric, $\tau_{up} = \tau_{dn}$.

and the RTN wave form is symmetric: compare Figs. 3 and 2.

The disappearance of differences between the background fluctuations around RTN levels at the symmetrizing current strongly suggests that the apparent differences in RTN background noise variances are associated with differences in RTN lifetimes at distinct metastable levels. This translates directly into differences in the effective bandwidth in which the background noise at each level is observed in the experiment. In the time domain the mean square noise around each RTN level is

$$\langle \sigma^2_{up(dn)} \rangle = \frac{1}{T} \int_0^T [U(t) - \bar{U}_{up(dn)}]^2 \, dt, \tag{1}$$

where $U(t)$ is the departure from the mean value $\bar{U}_{up(dn)}$ of the signal, and T is a time interval. On the other hand, in the frequency domain, the variance of a signal with a zero mean can be expressed as

$$\langle \sigma^2 \rangle = \int_{f_{min}}^{f_{max}} S(f) df, \tag{2}$$

where the bracket denotes ensemble averaging, $S(f)$ is the spectral density function (PSD). The maximum frequency in the record and the upper limit for the integral (2) is set by the data sampling frequency, $f_{max} = 1/\Delta t$, where Δt is the time interval between data points. The lower frequency limit of the experimental bandwidth is set by the inverse of the average RTN lifetime, $f_{min} = 1/\tau$.[23–25] To compare the real intensities of the background noise at distinct RTN level and to establish whether quiet and noisy metastable states exist in physical reality one should calculate the variance ratio directly from Eq. (2). This requires the functional form of the PSD for the background noise.

One can determine $S(f)_{bckgnd}$, assuming the RTN and background fluctuations are uncorrelated, by subtracting the PSD of a pure RTN contribution $S(f)_{rtn}$ from the total experimentally recorded $S(f)_{exp}$. For a pure two-level RTN signal,[26]

$$S(f)_{rtn} = 4 \Delta V^2 \frac{(\tau_{up} \tau_{dn})^2}{(\tau_{up} + \tau_{dn})^3} \frac{1}{1 + 4\pi^2 f^2/f_c^2}, \tag{3}$$

where $f_c = \tau_{up}^{-1} + \tau_{dn}^{-1}$. The spectrum of a pure RTN contribution can be calculated from Eq. (3), by inserting the amplitude ΔV, and average lifetimes τ_{up}, and τ_{dn} obtained from statistical analysis of the experimental time records. However, this approach cannot be applied to signals in which RTN and background fluctuations are correlated. In this case the spectrum $S(f)_{exp} = S(f)_{rtn} + S(f)_{bckgnd} + S(f)_{rtn,bckgnd}$ also contains an unknown cross-correlation term. In our experiments we find strong indications that RTN and background noise fluctuations may be correlated. Moreover, if quiet and noisy metastable states really exist it is quite plausible that the background noise at distinct RTN levels may be characterized by spectral densities not only with different intensities but also with different functional forms of $S(f)$. Thus to investigate RTN background noise problem one should create artificial time records representing background fluctuations at each RTN level and find their Fourier transforms. Noise records of the separate RTN levels can be obtained by redistributing the experimental record into two subsets, each containing only data points belonging to a given RTN state, as described in the next section.

III. RTN ANALYSIS IN TIME DOMAIN

The proposed analysis procedures are based on the assumption that the telegraph noise constitutes a discrete Marcovian dichotomous signal with Poisson statistics of the lifetime distribution and a single amplitude ΔV, while the fluctuations within telegraph levels are due only to the background noise which is assumed to be Gaussian.

In the experiment, the continuous signal $U(t)$ is sampled with a frequency $f_c = 1/\Delta t$ into a digital record $\{U_n\}$ of the length $N\Delta t$, containing N data points equally spaced in chronological order, $n = (1, 2, \ldots, N)$. First, we fit amplitude histogram $\{U_n\}$ to the two-Gaussian distribution $G(U_n)$ corresponding to the sum of background noise distributions around up and down RTN levels

$$G(U_n) = G_{dn}(U_n) + G_{up}(U_n)$$

$$= \frac{A_{dn}}{\sigma_{dn}\sqrt{2\pi}} e^{-(U_n - \bar{U}_{dn})^2/2\sigma_{dn}^2}$$

$$+ \frac{A_{up}}{\sigma_{up}\sqrt{2\pi}} e^{-(U_n - \bar{U}_{up})^2/2\sigma_{up}^2}, \tag{4}$$

where σ_{dn} and σ_{up} are the variances of the background noise around the mean values $\bar{U}_{dn}$ and $\bar{U}_{up}$, respectively, $A_{up} = N_{up}\Delta U$ and $A_{dn} = N_{dn}\Delta U$ are the areas under the Gaussian curves, ΔU is the size of the amplitude histogram bin, and N_{up} and N_{dn} stand for the total number of data points in the record belonging to the respective {up} and {dn} telegraph state. The probability that a data point from {up(dn)} takes a value $[U_n - \Delta U/2, U_n + \Delta U/2]$ is $G_{up(dn)}(U_n)[\Delta U/A_{up(dn)}]$. We start from a point $n-1$ that with the probability $\mathcal{P} = 1$ belongs to {dn}, i.e., $U_{n-1} \leqslant U_{min}^{up}$ (see Fig. 4). The probability that the next data point n, takes a value $U \epsilon [U_n - \Delta U/2, U_n + \Delta U/2]$ is given by a sum of the probabilities of two alternative events, $\mathcal{P}_{n_{\{dn\}}}^{up} + \mathcal{P}_{n_{\{dn\}}}^{dn}$, in which point n belongs to the state {dn} or {up}. The first term is the product of the probabilities that the point n takes a value from the
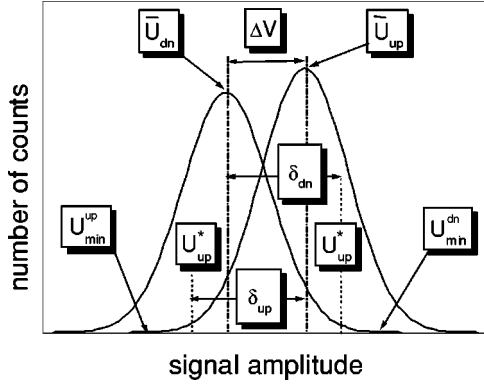
FIG. 4. Amplitude histogram of a noisy RTN signal. An example of overlapping Gaussian distributions described by Eq. (4).

range $[U_n - \Delta U/2, U_n + \Delta U/2]$ and that a transition from {dn} to {up} has occurred in the time between acquisition of the data points $n-1$ and n,

$$\mathcal{P}_{n_{\{dn\}}}^{up} = G_{up}(U_n)\frac{\Delta U}{A_{up}}\frac{\Delta t}{\tau_{dn}}. \qquad (5)$$

The second term describes the joint probability of an event in which point n takes the same value and no transition occurs between data points $n-1$ and n,

$$\mathcal{P}_{n_{\{dn\}}}^{dn} = G_{dn}(U_n)\frac{\Delta U}{A_{dn}}\left(1 - \frac{\Delta t}{\tau_{dn}}\right). \qquad (6)$$

A criterion for ascribing the data point n either to the state {up} or to the state {dn} can be based on comparing the probabilities (5) and (6). We define

$$\mathcal{F}_{dn}(U_n) = \frac{\mathcal{P}_{n_{\{dn\}}}^{up}}{\mathcal{P}_{n_{\{dn\}}}^{dn}} = \frac{G_{up}(U_n)}{G_{dn}(U_n)}\frac{A_{dn}\Delta t}{A_{up}(\tau_{dn} - \Delta t)}. \qquad (7)$$

Clearly, when $\mathcal{F}_{dn} > 1$ then $n \in \{up\}$, whereas for $\mathcal{F}_{dn} < 1$ $n \in \{dn\}$. In an analogous way, assuming that point $n-1$ belongs to the state {up}, we can formulate the probability of ascribing the data point n to either {up} or {dn},

$$\mathcal{F}_{up}(U_n) = \frac{\mathcal{P}_{n_{\{up\}}}^{dn}}{\mathcal{P}_{n_{\{up\}}}^{up}} = \frac{G_{dn}(U_n)}{G_{up}(U_n)}\frac{A_{up}\Delta t}{A_{dn}(\tau_{up} - \Delta t)}. \qquad (8)$$

For $\mathcal{F}_{up} > 1$ point $n \in \{dn\}$, whereas for $\mathcal{F}_{up} < 1$ we have $n \in \{up\}$. For practical convenience one may convert the probability criterion into the voltage criterion by solving equations $\mathcal{F}_{dn} = 1$ and $\mathcal{F}_{up} = 1$. The solutions, U_{dn}^* and U_{up}^*, respectively, determine the threshold voltages (see Fig. 4) which can be employed for fast redistribution of the acquired data points between the RTN states. If the previously analyzed point has been attributed to the state {dn} then the next data point will be ascribed to the same state if $U_n \leq U_{dn}^*$, and to the opposite state otherwise. If a data point $n-1$ was ascribed to the state {up} then the point n will belong to the same state when $U_n \geq U_{up}^*$.

To determine the threshold voltages one needs to know A_{up} and A_{dn}, $\bar{U}_{up}$ and $\bar{U}_{dn}$, σ_{up} and σ_{dn}, and the average lifetimes τ_{up} and τ_{dn}. All but τ_{up} and τ_{dn} are already known

from the initial fit of the experimental amplitude histograms to a two-Gaussian distribution (4). The missing average RTN lifetimes can be determined through a conventional statistical analysis of lifetime distributions or, alternatively, evaluated from the areas under the relevant Gaussian curve, provided that the total number of transition in the record k is known. In a large k approximation, $k \gg 1$, the average RTN lifetimes can be approximated by

$$\tau_{up(dn)} = \frac{2}{k}\frac{A_{up(dn)}}{\Delta U}\Delta t. \qquad (9)$$

The total number of transitions in the experimental record is usually large and the approximation $k \gg 1$ is generally well justified, nevertheless, the total number of transitions in the record is still not known. The missing k value can be determined by tentatively redistributing data points according to a simplified rough criterion, which does not require the knowledge of average lifetimes, and subsequently performing iterative fitting procedures of thus redistributed records to the original experimental Gaussian distributions.

In the approximation $\sigma_{up} = \sigma_{dn} = \sigma$. Equations (8) and (7) have the following solutions:

$$U_{dn}^* = \frac{\bar{U}_{dn} + \bar{U}_{up}}{2} + \frac{\sigma^2}{\Delta U}\ln\left(\frac{\tau_{dn}}{\Delta t} - 1\right) = \bar{U}_{dn} + \delta_{dn}, \qquad (10)$$

$$U_{up}^* = \frac{\bar{U}_{dn} + \bar{U}_{up}}{2} - \frac{\sigma^2}{\Delta V}\ln\left(\frac{\tau_{up}}{\Delta t} - 1\right) = \bar{U}_{up} - \delta_{up}. \qquad (11)$$

A rough criterion for the zero-order redistribution of data points can be established by setting the logarithmic terms to unity. The resulting approximate, overestimated voltage criteria read

$$\tilde{U}_{dn}^* = \bar{U}_{dn} + \frac{\Delta V}{2} + \frac{\sigma^2}{\Delta U}, \qquad (12)$$

$$\tilde{U}_{up}^* = \bar{U}_{up} + \frac{\Delta V}{2} - \frac{\sigma^2}{\Delta U}. \qquad (13)$$

After an initial tentative redistribution of data points from the experimental record one can build an artificial time record of a pure RTN and easily count the number of telegraph transitions k_0. Using k_0 as a zero order approximation of the real k, one calculates τ_{up} and τ_{dn} using Eq. (9). Next, the separation procedure is again performed, this time with the help of the exact criteria (8) and (7), whichever is appropriate. Subsequently, the new, corrected pure RTN record is created and the new number of transitions, k_1, is counted. The iterations are repeated i times, until the final number of transitions $k_i = k$ is obtained. The final k_i is the value for which Gaussian distributions around each RTN state, as obtained through the separation procedures, fit to the original experimental distributions $G_{up}(U)$ and $G_{dn}(U)$. The described procedure converges rapidly and typically $i < 5$ iterations are needed to obtain a stable k and calculate the values of τ_{up} and τ_{dn}.

The proposed procedure works well even for relatively noisy RTN signals, as illustrated in Fig. 5 showing a ''noisy'' RTN signal together with a record of clean telegraph contribution revealed by means of the above described
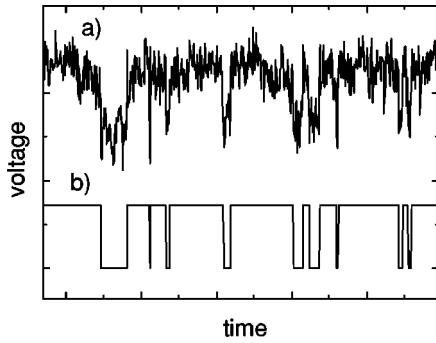
FIG. 5. Results of the analysis of a noisy RTN signal in the time domain according to the proposed technique. Shown is (a) original experimental time record, (b) pure RTN component inferred from the experimental record.

procedure. Note that all telegraph jumps, even those strongly perturbed by the background noise, can be seen in the pure RTN record. The pure RTN record can be also employed as a guide to extract artificial separate records of background noise at each RTN level from the data.

IV. RESULTS AND DISCUSSION

The knowledge of the RTN average lifetimes, see Fig. 3, determined by statistical analysis of the time record, and the acquisition rate allowed us to determine the effective bandwidth for the background noise. Now, we have to determine the functional form of the background noise spectra. For that purpose, using the procedures described above, we created an artificial time record of a pure RTN contribution and a record containing only the background noise components. The background noise record was obtained by subtracting, in the time domain, the pure telegraph contribution from the total experimental record. Subsequently, for each current, we calculated the spectral densities of background noise records. An example of such analysis for a current close to I_s is shown in Fig. 6. The pure RTN contribution has a Lorentzian shape described by Eq. (3), while the background noise power spectrum follows a $1/f^{0.5}$ power law within the experimental frequency range. We have verified by further separation of the background noise time record into two separate contributions corresponding to the {up} and {down} RTN states that all the background noise components are characterized by the same $1/f^{0.5}$ PSD. Moreover, this functional form of the PSD does not change with changing current within the entire noisy window range.

By inserting $S(f,I) = C(I)/f^{0.5}$ into Eq. (2) we obtain the background noise variance at a given RTN level

$$\langle \sigma^2 \rangle = \int_{1/\tau(I)}^{1/\Delta t} S(f,I) df = \int_{1/\tau(I)}^{1/\Delta t} \frac{C(I)}{f^{0.5}} df$$

$$= C(I) \left[1 - \left(\frac{2\Delta t}{\tau(I)} \right)^{0.5} \right], \quad (14)$$

where $C(I)$ is a current dependent constant characterizing the noise intensity at a unit frequency and τ is the average lifetime at the considered RTN level. We proceed by calculating, for each current, the ratio between variances at two
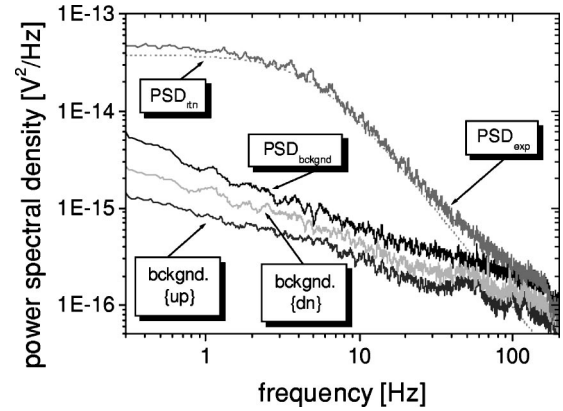

FIG. 6. Spectral densities of the total experimental record PSD_{exp}, of the pure RTN component PSD_{rtn}, and of the background noise PSD_{bckgnd} for currents close to I_s. The spectral density of a pure RTN wave has been calculated from Machlup's formula (3) using statistically averaged values obtained from the discussed time domain analysis. The PSD_{bckgnd} is further divided into constituent components related to {dn} and {up} telegraph states. The down and up background noise components shown are evaluated from the artificial time records containing only data points belonging to the relevant RTN state (separate spectral components of the background noise are not normalized to the record length). Note that all components of the background noise follow the same $1/\sqrt{f}$ frequency dependence.

RTN levels using Eq. (14) with $\tau(I)$ values determined from the statistical analysis of the pure RTN wave form

$$\frac{\langle \sigma_{dn}^2 \rangle}{\langle \sigma_{up}^2 \rangle} = \frac{C_{dn}(I)}{C_{up}(I)} \frac{\left[1 - \left(\frac{2\Delta t}{\tau_{dn}(I)} \right)^{0.5} \right]}{\left[1 - \left(\frac{2\Delta t}{\tau_{up}(I)} \right)^{0.5} \right]}. \quad (15)$$

At this point we arrive at the crucial question about the real intensities of the background noise around RTN levels, C_{up} and C_{dn}. Let us, for a moment, assume that the noise intensities on both levels are equal $C_{up}/C_{dn} = 1$. The variance ratio calculated from Eq. (15) under the assumption of identical background noise intensities on both RTN levels, is
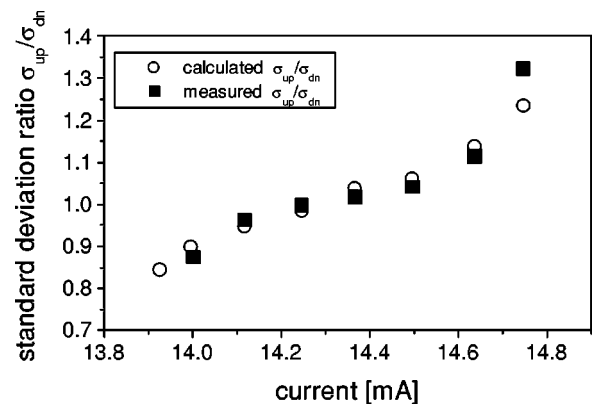

FIG. 7. Variance ratio of the background noise around up and down RTN states calculated according to Eq. (2), solid circles, compared with the variance ratio obtained from the Gaussian distributions of the experimental data, filled squares.
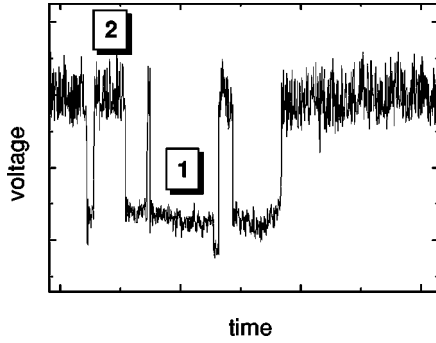
FIG. 8. RTN record demonstrating noisy metastable state in a short pulse.

compared with the experimental variance ratio determined from the width of the Gaussian background noise distributions in Fig. 7. The agreement between the calculated and experimental results is excellent, indicating that the background noise intensities on both RTN levels are indeed identical. Therefore, we conclude that the difference in the background noise traces, appearing as quiet and noisy metastable states, is not due to the exotic structure of a two-level fluctuator but results from the bandwidth limits imposed on the observable background noise by the telegraph fluctuations.

It is worth emphasizing that it is the RTN mean lifetime that determines the experimental bandwidth, and consequently noise variance at a given level, and not the individual pulse duration. This feature is clearly seen in Fig. 8 showing a fragment of a time record demonstrating the effect of quiet and noisy RTN states. For this record $\tau_{\rm up} > \tau_{\rm dn}$, and voltage fluctuations around the up level appear to be much stronger than those around the down level. Our claim that the difference in background noise at two RTN levels is due to a different bandwidth in which we observe fluctuations around a given state translates into the length of the time window in which a given state is observed. One may then ask why are the fluctuations within the pulse labeled as ''1'' in Fig. 8 smaller than the fluctuations of the pulse labeled ''2,'' if the length of the pulse ''1'' $t_{\rm dn}^1$ is clearly longer than the lifetime $t_{\rm up}^2$ of the pulse ''2.'' Since the time during which we observe pulse 1 is longer, therefore also the bandwidth should be wider and the fluctuations around 1 should be stronger then those around 2. This does not happen because RTN noise constitutes a Markovian process without a memory. When the RTN switches to another level, the only information available to the system is the probability of switching back to the previous state given by the inverse of the statistically average RTN lifetime. As our system does not know how long it will stay in a given state, the variance at a given level cannot adjust itself to the actual pulse length but only to the statistically significant variable, i.e., to the average lifetime. Remember that RTN lifetimes (pulse lengths) are exponentially distributed. Therefore one may well encounter a long pulse belonging to the distribution with a short average lifetime as well as a short pulse from the distribution characterized by a long average lifetime. Consequently, fluctuations around a shorter pulse with a longer average lifetime will appear stronger than those around a longer pulse with a short average lifetime, as is the case illustrated in Fig. 8.

V. CONCLUSIONS

We conclude that, at least in our experimental case, quiet and noisy metastable states do not exist. The difference between fluctuations around distinct RTN levels, so clearly visible in the experimental time records, is due only to the differences in the effective bandwidth in which one the background noise is seen in the experiments. The bandwidth limits are imposed by the signal sampling rate and the average lifetimes of the random telegraph signal. The observed changes of the variance ratio with changing current result from the current dependence of the RTN lifetimes.

We emphasize that to claim that quiet and noisy metastable states really exist in the reality it is not enough to detect different noise variances around different RTN levels. The proper conclusion can be drawn only after different background fluctuations appear in a symmetric RTN wave form, for which the background noise bandwidth at both RTN levels is the same. In the pioneering experiments on flux noise this was clearly not the case in the entire temperature range investigated as it follows from the evaluations of the average RTN lifetimes.[5] Nevertheless, in these zero field and zero current experiments it was not possible to change the pristine symmetry of the observed RTN signal and to establish if the quiet and noisy metastable states are due to bandwidth differences or reflect a real exotic structure of the involved two-level fluctuator. In our early communique[16] concerning amplitude modulated RTN voltages in thin HTSC films we suggested the possible existence of statistical correlations between the RTN and background noise components based on appearances of quiet and noisy metastable states. Unfortunately, we completely disregarded the fact that noise variances around RTN levels were actually equal for a symmetric RTN signal. The quiet and noisy metastable states as reported in Ref. 16 are therefore most likely also due to the noise bandwidth limits that change with changing bias current. However, the real quiet and noisy metastable states may exist in the RTN events reported recently in Ref. 27.

Finally, we consider why different RTN background noise levels are so rarely observed experimentally. If the bandwidth limiting mechanism is correct, one would expect to see quiet and noisy metastable states in all asymmetric RTN manifestations. The answer lies in the particular functional form of the background noise. Note that the bandwidth differences have little influence on the variance ratio when the background noise is white. It follows from Eq. (2) that for white background noise with spectral density $C(I)$

$$\frac{\langle \sigma_{\rm dn}^2 \rangle}{\langle \sigma_{\rm up}^2 \rangle} = \frac{C_{\rm dn}(I)}{C_{\rm up}(I)} \frac{(1/\Delta t) - 1/\tau_{\rm dn}}{(1 \Delta t) - 1/\tau_{\rm up}}. \tag{16}$$

Since the sampling rate $1/\Delta t$ has to satisfy $\Delta t \ll \tau_{\rm up}, \tau_{\rm dn}$, for the white background noise $\langle \sigma^2 \rangle_{\rm dn} / \langle \sigma^2 \rangle_{\rm up} \approx 1$. Background noise with $1/f^\alpha$-like spectrum clearly exercises a much stronger influence on the variance ratio. In fact, only this type of background noise can give rise to experimentally observable quiet and noisy metastable states.

---

*Also at Instytut Fizyki PAN, Al. Lotników 32, PL 02-668 Warszawa, Poland.

[1] J.R. Clem, Phys. Rep. **75**, 1 (1981).

[2] B. Placais, P. Mathieu, and Y. Simon, Phys. Rev. B **49**, 15 813 (1994).

[3] G. Jung and B. Savo, J. Appl. Phys. **80**, 2939 (1996).

[4] Sh. Kogan, *Electronic Noise and Fluctuations in Solids* (Cambridge University Press, Cambridge, 1996).

[5] M.J. Ferrari, Mark Johnson, F.C. Wellstood, J.J. Kingston, T.J. Shaw, and John Clarke, J. Low Temp. Phys. **94**, 15 (1994).

[6] T.S. Lee, N. Missert, L.T. Sagdhal, John Clarke, J.R. Clem, K. Char, J.N. Eckstein, D.K. Fork, L. Lombardo, A. Kapitulnik, L.F. Shneemayer, J.V. Waszczak, and R.B. van Dover, Phys. Rev. Lett. **74**, 2796 (1995).

[7] S.A.L. Foulds, J. Smithyman, G.F. Cox, C.M. Muirhead, and R.G. Humphreys, Phys. Rev. B **55**, 9098 (1997).

[8] E. Shung, T.F. Rosenbaum, S.N. Coppersmith, G.W. Crabtree, and W. Kwok, Phys. Rev. B **56**, R11431 (1997).

[9] R. Buder, J. Dumas, C. Escribe-Filippini, H. Guyot, Ch. J. Liu, J. Markus, S. Revenaz, P. L. Reydet, and C. Schlenker, in *Studies of High Temperature Superconductors*, edited by A. Narlikar (Nova Science Publishers, New York, 1990), Vol. **7**, p. 223.

[10] G. Jung, S. Vitale, J. Konopka, and M. Bonaldi, J. Appl. Phys. **70**, 5440 (1991).

[11] G. Jung, B. Savo, and A. Vecchione, Europhys. Lett. **21**, 947 (1993).

[12] E.R. Nowak, N.E. Israeloff, and A.M. Goldman, Phys. Rev. B **49**, 10 047 (1994).

[13] L.B. Kiss and P. Svendlindh, IEEE Trans. Electron Devices **41**, 2112 (1994).

[14] M. Bonaldi, G. Jung, B. Savo, A. Vecchione, and S. Vitale, Phys. Rev. B **53**, 90 (1996).

[15] G. Jung, B. Savo, A. Vecchione, I. Khalfin, and B.Ya. Shapiro, in *Superconductivity and Particle Detection*, edited by T. Girard, A. Morales, and G. Waysand (Word Scientific, Singapore, 1995), p. 291.

[16] G. Jung, B. Savo, and C. Coccorese, in *Applied Superconductivity*, edited by D. Dew Huges (Institute of Physics Publishing, Bristol, 1996), p. 1003.

[17] G. Jung, Y. Yuzhelevski, B. Savo, C. Coccorese, V.D. Ashkenazy, and B.Ya. Shapiro, in *Unsolved Problems of Noise*, edited by Ch.R. Doering, L. Kiss, and M.F. Shlesinger (World Scientific, Singapore, 1997), p. 285.

[18] R.T. Wakai and D.J. Van Harlingen, Phys. Rev. Lett. **58**, 1687 (1987).

[19] M.J. Kirton and M.J. Uren, Adv. Phys. **38**, 367 (1989).

[20] K.R. Farmer, C.T. Rogers, and R.A. Burhman, Phys. Rev. Lett. **58**, 2255 (1987).

[21] K.S. Ralls and R.A. Burhman, Phys. Rev. Lett. **60**, 2434 (1988).

[22] C. Attanasio, C. Coocorese, L. Maritato, M. Salluzzo, and M. Slavato, Nuovo Cimento D **16**, 1961 (1984).

[23] T.G.M. Kleinpenning and A.H. de Kuijper, J. Appl. Phys. **63**, 43 (1988).

[24] U.J. Strasilla and M.J.O. Strutt, J. Appl. Phys. **46**, 1423 (1974).

[25] T.G.M. Kleinpenning, Physica B **164**, 331 (1990).

[26] S. Machlup, J. Appl. Phys. **25**, 341 (1954).

[27] B. Savo and C. Coccorese, IEEE Trans. Appl. Supercond. **9**, 2336 (1999).